

Probing non-Hermitian phase transitions in curved space via quench dynamics

Ygor Pará,¹ Giandomenico Palumbo,² and Tommaso Macrì^{1,3}

¹Departamento de Física Teórica e Experimental, Universidade Federal do Rio Grande do Norte, 59072-970 Natal-RN, Brazil*

²School of Theoretical Physics, Dublin Institute for Advanced Studies, 10 Burlington Road, Dublin 4, Ireland†

³International Institute of Physics, Universidade Federal do Rio Grande do Norte, 59078-400 Natal-RN, Brazil‡

Non-Hermitian Hamiltonians are relevant to describe the features of a broad class of physical phenomena, ranging from photonics and atomic and molecular systems, to nuclear physics and mesoscopic electronic systems. An important question relies on the understanding of the influence of curved background on the static and dynamical properties of non-Hermitian systems. In this work, we study the interplay of geometry and non-Hermitian dynamics by unveiling the existence of curvature-dependent non-Hermitian phase transitions. We investigate a prototypical model of Dirac fermions on a sphere with an imaginary mass term. This exactly-solvable model admits an infinite set of curvature-dependent pseudo-Landau levels. We characterize these phases by computing an order parameter given by the pseudo-magnetization and, independently, the non-Hermitian fidelity susceptibility. Finally, we probe the non-Hermitian phase transitions by computing the (generalized) Loschmidt echo and the dynamical fidelity after a quantum quench of the imaginary mass and find singularities in correspondence of exceptional radii of the sphere.

I. INTRODUCTION

Non-Hermitian (NH) topological systems have become a very active and prolific research field in recent years [1–10]. This is due to the their novel and peculiar physical features such as the NH skin effect [11–14] and the lacking of the conventional bulk-edge correspondence [15–19], as well as to the plethora of experimental platforms where these systems can simulated and tested. A special class of non-Hermitian phases is defined by the \mathcal{PT} (parity and time reversal (TR)) symmetry, where the spectrum is completely real even with the absence of the Hermitian condition [20, 21]. This symmetry is important also because NH phase transitions are deeply related to the existence of the exceptional points (EPs) [22–26], which are associated to the critical phase transitions between \mathcal{PT} -symmetric and \mathcal{PT} -broken phases. These special points are characterized by topological invariants [27]. Moreover, the presence of EPs can be tested at dynamical level by employing genuine information-theoretic quantifiers such as (generalized) fidelities and Loschmidt echos [28–32]. Notice, these powerful theoretical tools have been largely used in the study of Hermitian phase transitions [32–47].

However, differently from Hermitian systems, the behavior of NH phases is still poorly understood on curved background. Curved space for emergent relativistic fermions in condensed matter physics can be associated, for instance, to the physical curvature of 1D, 2D and 3D materials, to effective geometry created from the synthetic matter or to formal geometric approaches employed to study the quantum thermal effects in topological phases [48–65]. Importantly, it has also been shown that curved background can give rise to genuine Hermitian phase transitions [66–69].

The main goal of our work is to unveil the existence of curvature-dependent non-Hermitian phase transitions. These non-Hermitian phases are characterized by EPs which depend on the geometry of the system. In particular, these *geometric* EPs exist only on curved space and in general are hard to identify and describe due to the lack of translation symme-

try. For this reason, we will present and study a prototypical analytical solvable model in two dimensions given by Dirac fermions on the sphere. In the Hermitian case, this model arises in fullerene [70–76] and as a surface model of three-dimensional topological insulators [77–79]. Importantly, experimental realizations with superconducting resonators [80] and topological nanoparticles [81, 82] recently appeared. We will induce NH phases by introducing a complex Dirac mass, which can be implemented by introducing on-site gain and/or loss similarly to the flat case [7, 16, 83–86]. This situation render the Hamiltonian always intrinsically non-Hermitian [87] inducing exceptional points in the energy spectrum.

Firstly, we will analytically solve the model by showing the emergence of NH pseudo-Landau levels and their discrete symmetries. Notice, these pseudo-Landau levels are related to the intrinsic curvature of the sphere and are the analog of pseudo-Landau levels induced in flat space through strain [88–95].

Secondly, we will present the infinite sequence of geometric EPs, which will directly depend on the radius (curvature) of the sphere and relate the static properties of the spectrum through a pseudo-magnetization induced by the imaginary Dirac mass.

Finally, we will employ quench dynamics to characterize these curvature-dependent NH phase transitions. In particular, we will show that the NH versions of the Loschmidt echo and fidelity [31] are able to distinguish between the different phases of the model. The existence of non-analytic points in the fidelity will represent the clear signature of the presence of the geometric EPs. This will be performed by quenching the imaginary mass term and tuning the radius of the sphere to different values.

II. MODEL

We consider the dynamics of relativistic fermions constrained to the surface of a sphere of radius R . We will

induce Non-Hermitian phases by introducing an imaginary Dirac mass, which can be implemented by introducing on-site gain and/or loss similarly to the flat case [7, 16, 83–86]. The Dirac equation in 2+1 dimensions for a fermion of *complex* mass $\mu = M + i\Gamma$ (with both M and Γ real dimension-full constants) in a curved background is described by a two-component spinor $\Psi(\mathbf{x})$ reads [96–99]

$$(i\hbar\bar{\gamma}^\nu\nabla_\nu + \mu c)\Psi(\mathbf{x}) = 0. \quad (1)$$

The space-time coordinates are labeled by $\mathbf{x} = (ct, \theta, \phi)$, the covariant derivative is given by $\nabla_\nu = \partial_\nu + \frac{1}{8}\omega_{\nu bc}[\gamma^b, \gamma^c]$. The spin connection $\omega_{\mu b}^d = e_\nu^d(e_\sigma^b\Gamma^\nu{}_{\sigma\mu} + \partial_\mu e^\nu_b)$ is written in terms of the metric connection $\Gamma^\nu{}_{\sigma\mu} = \frac{1}{2}g^{\beta\nu}(\partial_\mu g_{\sigma\beta} - \partial_\beta g_{\sigma\mu} + \partial_\sigma g_{\mu\beta})$. We are using a, b, \dots for local frame indices and μ, ν, \dots for coordinate indices. The metric of this space is $g_{\mu\nu} = \text{diag}(1, -R^2, -R^2 \sin^2 \theta)$, with determinant $g = R^4 \sin^2 \theta$. The *vielbein* is given by the definition $g_{\mu\nu} = \eta_{ab}e_\mu^a e_\nu^b$, where $\eta_{ab} = \text{diag}(1, -1, -1)$. We also defined the inverse *vielbein* to satisfy $e_\mu^a e^\mu_b = \delta_a^b$. We write the gamma matrices as $\bar{\gamma}^\mu = e^\mu_a \gamma^a$, where we choose $\gamma^0 = \sigma_z$, $\gamma^1 = -i\sigma_x$, $\gamma^2 = -i\sigma_y$, consistently with the anti-commutation relations $\{\bar{\gamma}^\mu, \bar{\gamma}^\nu\} = 2g^{\mu\nu}$ [100].

The massless case represents the effective low-energy model for the some spherical condensed matter systems such as fullerene and the boundary states of spherical topological insulators [70–75, 77–79, 101–103]. It has also been employed in the prediction of some spectral properties related to the number of zero modes, which are theoretically predicted by the Atiyah-Singer index theorem [76, 80]. In the context of three-dimensional topological insulators, the model in Eq.(1) displays several many-body phases in presence of attractive and in repulsive interactions [104].

By separating the time component from the spatial ones in Eq. (1), we can write a Dirac Hamiltonian in the form

$$\hat{H}_\mu = \begin{pmatrix} -\mu c^2 & \frac{\hbar c}{R} \hat{h}^- \\ \frac{\hbar c}{R} \hat{h}^+ & \mu c^2 \end{pmatrix}, \quad (2)$$

with $\hat{h}^\pm = \pm(\partial_\theta + \frac{\cot\theta}{2}) + \frac{i}{\sin\theta}\partial_\phi$. It is important to note that due to the presence of the NH mass term $\hat{\Sigma}_z = -\mu c^2 \sigma_z$, Eq.(2) is a NH Hamiltonian, i.e. $\hat{H}_\mu \neq \hat{H}_\mu^\dagger$. The eigenvalues $E_{\mu,R}^{(n,m,\lambda)}$ of H_μ can be obtained by squaring the Hamiltonian \hat{H}_μ of Eq.(2)

$$E_{\mu,R}^{(n,m,\lambda)} = \lambda \sqrt{\frac{\hbar^2 c^2}{R^2} \Omega_{nm}^2 + \mu^2 c^4}, \quad (3)$$

where $\lambda = \pm 1$ and $\Omega_{nm} = n + |m| + 1/2$.

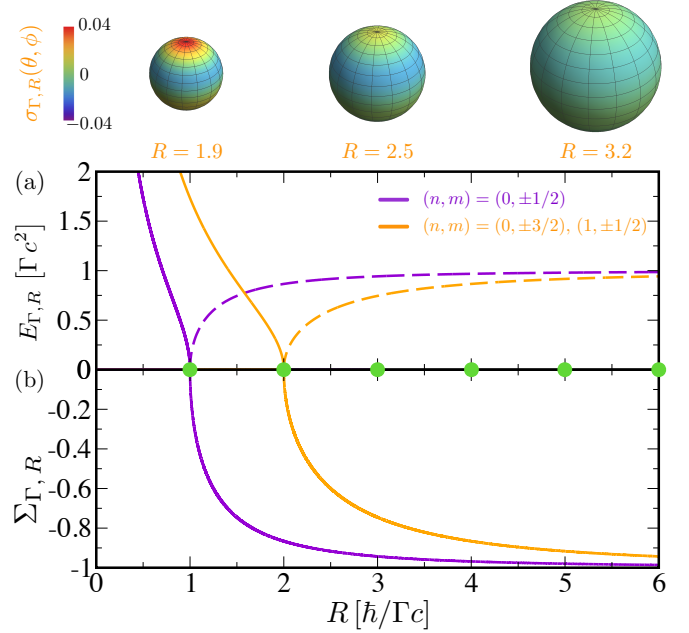


Figure 1. Eigenvalues and NH magnetization for the eigenstates of Eq.(1) as a function of the radius R of the sphere. (a) $E_{\Gamma,R}$ for $\lambda = 1$ in units of Γc^2 for the the first two pLLs with $(n,m) = (0, \pm 1/2)$ (purple) and $(1, \pm 1/2)$ (orange) in the TR-invariant region (real, full lines) and in the TR-broken phase (imaginary, dashed) according to Eq.(3). At the EPs (green circles) the eigenvalues have vanishing energy, and eigenstates with opposite signs coalesce with degeneracy $d = 4\Omega_{nm}$. (b) $\Sigma_{\Gamma,R}$ from Eq.(7) for $\lambda = 1$ and for the same pLLs of (a). At the EPs the spontaneous breaking of TR symmetry leads to a finite magnetization which asymptotically reaches the value $\Sigma_{\Gamma,\infty} = -1$. In the vicinity of the EPs $R \gtrsim R^*$, magnetization increases $\propto -\lambda(R - R^*)^{1/2}$. The energies and magnetizations for $\lambda = -1$ have opposite signs of $E_{\Gamma,R}$ and $\Sigma_{\Gamma,R}$. Top: Local magnetization $\sigma_{\Gamma,R}(\theta, \phi)$ across the EP at $R^* = 2$ for $(n,m,\lambda) = (1, 1/2, 1)$. For $R < R^*$, $\sigma_{\Gamma,R}(\theta, \phi) = -\sigma_{\Gamma,R}(\pi - \theta, \phi)$. For $R > R^*$, $\sigma_{\Gamma,R}(\theta, \phi)$ varies over a smaller range, and its integral is negative.

The indices n, m are respectively a positive integer and a half-integer, which label the pseudo-Landau levels (pLLs) of the model [105–108]. In the following we will focus on the case where the mass is purely imaginary, i.e. $\mu \equiv i\Gamma$. For this choice, an infinite set of EPs occur when $E_{\Gamma,R}^{(n,m,\lambda)} = 0$, i.e. $R\Gamma c^2 = \hbar c \Omega_{nm}$ with degeneracy $d = 4\Omega_{nm}$. At the EPs a pair of opposite-sign eigenvalues, connected by a square root branch point, coalesce [109, 110]. The evolution of the eigenvalues for the first pLLs are shown in Fig.(1)a as a function of the sphere radius R . The EPs are located at $R = R^*$, with $R^* = 1, 2$ respectively. For $0 < R < R^*$ the eigenvalues are real, whereas for $R > R^*$ they are imaginary.

We notice that the two-component spinor eigenvectors $\phi_{\Gamma,R}^{(n,m,\lambda)}(\theta, \phi)$ of \hat{H}_Γ have a nonvanishing scalar product

$$\int_0^\pi \int_0^{2\pi} \left(\phi_{\Gamma,R}^{(n_1,m_1,\lambda_1)} \right)^\dagger \phi_{\Gamma,R}^{(n_2,m_2,\lambda_2)} \sqrt{|g|} d\phi d\theta = C_{\lambda_1,\lambda_2} \delta_{n_1,n_2} \delta_{m_1,m_2}, \quad (4)$$

with $C_{\lambda_1,\lambda_2} \neq 0$ for any nonzero value of Γ , and therefore

they form a non-orthogonal basis [111, 112]. The prefactor of $\phi_{\Gamma,R}^{(n,m,\lambda)}(\theta, \varphi)$ is fixed by the requirement that the normalization constant is unitary. See the Appendix A for a detailed derivation of the spectrum.

A. Discrete symmetries

The time reversal (TR) operator is described by $\mathcal{T} = -i\sigma_y K$, where K is the usual complex conjugation. The massless Dirac Hamiltonian \hat{H}_0 in Eq.(2) with $\Gamma = 0$ is Hermitian, and it is simultaneously invariant under the action of both the parity and TR symmetry [49, 78, 104, 113, 114]. Any finite (real or complex) mass breaks parity symmetry. Conversely, the Hamiltonian \hat{H}_Γ is invariant under TR symmetry. We also notice that, in our relativistic formulation, TR acts in a similar fashion as a combined \mathcal{PT} -symmetry for a single spin system with no center-of-mass dynamics [20]. The TR operator \mathcal{T} acts on the eigenstates $\phi_{\Gamma,R}^{(n,m,\lambda)}$ of \hat{H}_Γ as follows

$$\mathcal{T}\phi_{\Gamma,R}^{(n,m,\lambda)} = \begin{cases} (-1)^{m-\frac{1}{2}}\phi_{\Gamma,R}^{(n,-m,\lambda)} & \text{for } \hbar c \Omega_{nm} > R\Gamma c^2 \\ (-1)^{m-\frac{1}{2}}\phi_{\Gamma,R}^{(n,-m,-\lambda)} & \text{for } \hbar c \Omega_{nm} < R\Gamma c^2 \end{cases}. \quad (5)$$

Importantly, upon crossing any EPs, such that $R\Gamma c^2 > \hbar c \Omega_{nm}$ the effect of \mathcal{T} is to map an eigenstate $\phi_{\Gamma,R}^{(n,m,\lambda)}$ into an eigenstate $\phi_{\Gamma,R}^{(n,-m,-\lambda)}$ with opposite energy ($\lambda \rightarrow -\lambda$). Therefore an adiabatic variation of the radius (geometry) or the imaginary mass (gain and/or loss) across an EP *spontaneously* breaks TR symmetry. The TR symmetry due to Kramers' degeneracy, the real eigenvalues are always paired and can be split into two complex eigenvalue pairs (E, E^*).

The parity operator, equivalent to space reflection in $2+1$ dimensions, can be written as $\mathcal{P} = \sigma_z P_\theta$, where P_θ takes $\theta \rightarrow \pi - \theta$. But, the role of the proper parity operator in the model is played by the operator \mathcal{P}_0 which maps $\psi(\theta, \varphi) \rightarrow i\sigma_z \psi(\pi - \theta, -\varphi)$. This operator corresponds to a rotation around the z -direction in the spin degree of freedom and to a reflection with respect to the origin in the spatial coordinates. Combined with the TR operator satisfies indeed $(\mathcal{T}\mathcal{P}_0)^2 = 1$. The proof makes use of the properties of Jacobi polynomials and algebraic manipulations of the spinor under the transformations above. Also $\mathcal{T}\mathcal{P}_0$ signals the presence of the \mathcal{PT} -transition, as in the symmetric phase the eigenstates of the Hamiltonian are also eigenstates of $\mathcal{T}\mathcal{P}_0$. Instead, in the broken phases the eigenstates are no more eigenstates of $\mathcal{T}\mathcal{P}_0$, in a analogy to the usual \mathcal{PT} -transition.

B. Biorthogonal basis.

Several properties of a NH system can be obtained by the use of the biorthogonal basis. The eigenstates of \hat{H}_Γ^\dagger satisfy the eigenvalue equation $\hat{H}_\Gamma^\dagger \chi_{nm}^{(\lambda)} = \Xi_{nm}^{(\lambda)} \chi_{nm}^{(\lambda)}$. Note that the Hamiltonians \hat{H}_Γ and \hat{H}_Γ^\dagger differ only by the sign of Γ . The eigen-

values are related by $\Xi_{\Gamma,R}^{(n,m,\lambda)} = [E_{\Gamma,R}^{(n,m,\lambda)}]^*$. The eigenvectors of \hat{H}_Γ^\dagger are given by lengthy expressions reported in Appendix B. The set of the eigenstates of \hat{H}_Γ and \hat{H}_Γ^\dagger form a biorthogonal basis with a metric-dependent scalar product defined as [115–119]

$$\int_0^\pi \int_0^{2\pi} \left[\chi_{\Gamma,R}^{(n_1,m_1,\lambda_1)} \right]^\dagger \psi_{\Gamma,R}^{(n_2,m_2,\lambda_2)} \sqrt{|g|} d\varphi d\theta = \delta_{n_1,n_2} \delta_{m_1,m_2} \delta_{\lambda_1,\lambda_2}. \quad (6)$$

III. RESULTS

A. Magnetic phases

Based on the analysis of TR symmetry, and the analogy with usual magnetic systems, we expect the system to develop a spontaneous magnetization across an EP [120, 121]. Given a general spinor $\Phi = (\phi_\uparrow \ \phi_\downarrow)^\top$ we define a NH magnetization as $\Sigma_{\Gamma,R} = \int_0^{2\pi} \int_0^\pi \sigma_{\Gamma,R}(\theta, \varphi) \sqrt{|g|} d\theta d\varphi$, where $\sigma_{\Gamma,R}(\theta, \varphi) = (\phi_\uparrow^* \phi_\uparrow - \phi_\downarrow^* \phi_\downarrow)$ is the local magnetization (see top panel of Fig.(1)) [104]. For an eigenstate $\phi_{\Gamma,R}^{(n,m,\lambda)}$ the NH magnetization can be computed analytically

$$\Sigma_{\Gamma,R}^{(n,m,\lambda)} = \frac{\frac{\hbar^2 c^2}{R^2} \Omega_{nm}^2 - \left| E_{\Gamma,R}^{(n,m,\lambda)} + i\Gamma c^2 \right|^2}{\frac{\hbar^2 c^2}{R^2} \Omega_{nm}^2 + \left| E_{\Gamma,R}^{(n,m,\lambda)} + i\Gamma c^2 \right|^2}. \quad (7)$$

In Fig.(1)b we plot the magnetization for the PLL as a function of R . For $R < R^*$ the magnetization vanishes. At the critical radius $R = R^*$ the system develops a spontaneous magnetization. In the vicinity of an EP, with $R \gtrsim \hbar c \Omega_{nm}/\Gamma c^2$, we can expand Eq.(7) to obtain

$$\Sigma_{\Gamma,R}^{(n,m,\lambda)} \Big|_{R \gtrsim R^*} \approx -\lambda \sqrt{2} \left(\frac{R - R^*}{R^*} \right)^{\frac{1}{2}}, \quad (8)$$

where $R^* = \hbar \Omega_{nm}/\Gamma c$ is the critical radius. Therefore the magnetization signals the presence a second-order phase transition with a critical exponent $\beta = 1/2$, analogous to the mean-field critical exponent of the (Hermitian) Ising transition. Asymptotically, for $R \rightarrow \infty$ the magnetization saturates to $\Sigma_{\Gamma,\infty} = -\lambda$ depending on the sign of the energy eigenvalue. We emphasize that the NH magnetization $\Sigma_{\Gamma,R}^{(n,m,\lambda)}$ defined in Eq.(7) relies on the use of the non-orthogonal basis $\{\phi_{\Gamma,R}^{(n,m,\lambda)}(\theta, \varphi)\}$. Note that if we define NH magnetization using the biorthogonal basis and redefining appropriately the Pauli matrices [115, 116], the result is not sensitive to the EPs. To probe such NH phase transitions in curved space we will use other measurable quantities as described thoroughly in the following sections.

B. Fidelity susceptibility

A complementary approach to detect phase transitions *without* a previous knowledge of an order parameter is via the calculation of the fidelity susceptibility [33, 34, 36–39]. This approach has been recently generalized to the study of NH models [28–30]. Given two states $|\psi_{\Gamma_1}\rangle$, we define the NH fidelity is defined as [31]

$$\mathcal{F}_R\{|\psi_{\Gamma_1}\rangle, |\psi_{\Gamma_2}\rangle\} = \frac{|\langle\psi_{\Gamma_1}|\psi_{\Gamma_2}\rangle|^2}{\langle\psi_{\Gamma_1}|\psi_{\Gamma_1}\rangle\langle\psi_{\Gamma_2}|\psi_{\Gamma_2}\rangle}. \quad (9)$$

Notice that the scalar product $\langle\psi_{\Gamma_1,2}|\psi_{\Gamma_1,2}\rangle$ has to be computed at fixed λ and radius R , whereas other parameters (such as the mass Γ or time t) can vary between the two states. The denominator in Eq.(9) bounds the fidelity, $0 \leq \mathcal{F}_R \leq 1$. Given two states $|\psi_{\Gamma}\rangle$ and $|\psi_{\Gamma+\delta\Gamma}\rangle$, differing from an infinitesimal variation of the mass Γ one can define the nonorthogonal *static* fidelity susceptibility as

$$\chi_{\Gamma} = \lim_{\delta\Gamma \rightarrow 0} \frac{-\ln|\mathcal{F}_R\{|\psi_{\Gamma}\rangle, |\psi_{\Gamma+\delta\Gamma}\rangle\}|}{(\delta\Gamma)^2}. \quad (10)$$

In Fig.(2) we plot χ_{Γ} for the lowest pLL with $(n,m,\lambda) = (0, 1/2, 1)$. The susceptibility satisfies $\chi_{\Gamma} = \chi_{-\Gamma}$ and diverges at the EP when $\Gamma = \hbar\Omega_{n,m}/Rc$. In the inset of Fig.(2) we compute the scaling properties of χ_{Γ} around the EP at $\Gamma^* = 1$. Fitting the right (χ_{Γ}^+) and the left (χ_{Γ}^-) susceptibilities with the scaling functions $C_{\Gamma}^{\pm}|\Gamma - 1|^{\gamma}$ we find that $\gamma = 1$ with the same prefactor $C_{\Gamma}^{\pm} = 0.12$. Interestingly, we verified that the fidelity susceptibility has a qualitatively similar behavior adopting biorthogonal basis states. However the critical exponent γ is dependent on the choice of the basis states.

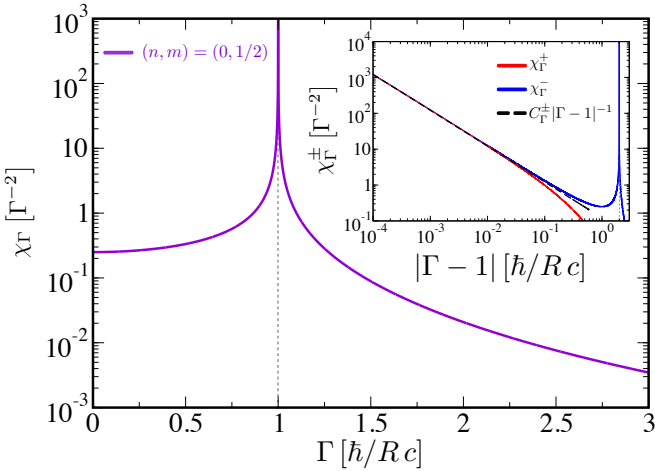


Figure 2. Fidelity susceptibility χ_{Γ} given by Eq. (10) of the lowest pLL for $n = 0$ and $m = 1/2$, as function of the mass Γ . Susceptibility χ_{Γ} diverges at the EP $\Gamma^* = \hbar\Omega_{0,1/2}/Rc$. χ_{Γ} is a symmetric function of Γ , i.e. $\chi_{\Gamma} = \chi_{-\Gamma}$. Scaling of χ_{Γ} approaching the EP from the right (red line) and from the left (blue). Both susceptibilities were fitted with the function $\chi_{\Gamma}^{\pm} = C_{\Gamma}^{\pm}|\Gamma - \Gamma^*|^{-1}$, with $C_{\Gamma}^{\pm} = 0.122$. The second peak of χ_{Γ}^- corresponds to the EP at $\Gamma = -\hbar\Omega_{0,1/2}/Rc$ outside the scaling region of the inset.

The fidelity susceptibility in the biorthogonal basis is defined as

$$\chi_{\Gamma}^{(B)} = \lim_{\delta\Gamma \rightarrow 0} \frac{-2\ln|F_{\Gamma}^{(B)}|}{(\delta\Gamma)^2}, \quad (11)$$

where $F_{\Gamma}^{(B)} = (\langle\chi_{\Gamma+\delta\Gamma,R}^{(n,m,\lambda)}|\psi_{\Gamma,R}^{(n,m,\lambda)}\rangle\langle\chi_{\Gamma,R}^{(n,m,\lambda)}|\psi_{\Gamma+\delta\Gamma,R}^{(n,m,\lambda)}\rangle)^{1/2}$ is the generalized Uhlmann fidelity computed on the eigenstates of \hat{H}_{Γ} and $\hat{H}_{\Gamma}^{\dagger}$ with the help of the biorthogonal basis [33].

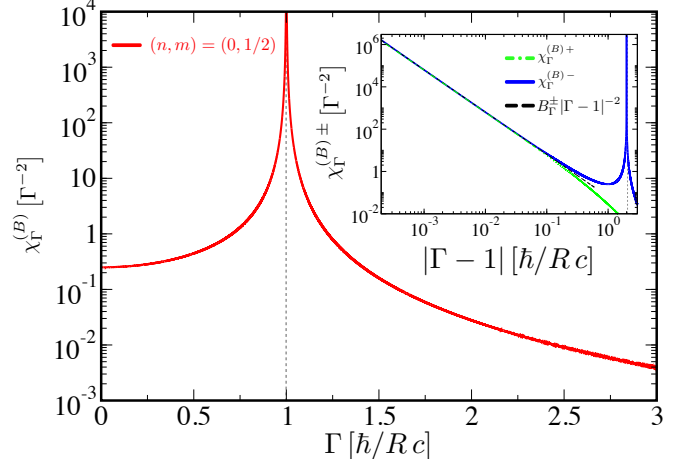


Figure 3. Biorthogonal fidelity susceptibility $\chi_{\Gamma}^{(B)}$ given by Eq. (11) of the lowest pLL for $n = 0$ and $m = 1/2$, as function of the mass Γ . Susceptibility χ_{Γ} diverges at the EP $\Gamma^* = \hbar\Omega_{0,1/2}/Rc$. $\chi_{\Gamma}^{(B)}$ is a symmetric function of Γ , i.e. $\chi_{\Gamma}^{(B)} = \chi_{-\Gamma}^{(B)}$. Inset. Scaling of $\chi_{\Gamma}^{(B)}$ approaching the EP from the right (red line) and from the left (blue). Both susceptibilities were fitted with the function $\chi_{\Gamma}^{(B)\pm} = B_{\Gamma}^{\pm}|\Gamma - \Gamma^*|^{-2}$, with $B_{\Gamma}^{\pm} = 0.064$. The second peak of $\chi_{\Gamma}^{(B)-}$ corresponds to the EP at $\Gamma = -\hbar\Omega_{0,1/2}/Rc$ outside the scaling region of the inset.

The biorthogonal fidelity $F_{\Gamma}^{(B)}$ generalizes to the NH case the distance between two quantum states for different values of the mass Γ . In Fig.(3) we plot $\chi_{\Gamma}^{(B)}$ for the lowest pLL of Eq.(1) as a function of Γ . The susceptibility diverges at the EP and it is symmetric under the exchange $\Gamma \rightarrow -\Gamma$. In the inset of fig.(3) we show that $\chi_{\Gamma}^{(B)}$ diverges quadratically approaching the EP, i.e. $\chi_{\Gamma}^{(B)} \propto |\Gamma - \Gamma^*|^{-\gamma/\gamma'}$ with $\gamma = \gamma' = 2$ the right/left susceptibility critical exponents.

C. Quench dynamics

We investigate the quantum evolution after a mass quench in the proximity of EPs. We monitor the effect on the dynamics of a rapid variation of the mass from Γ_i to Γ_f via the (time-dependent) fidelity $\mathcal{F}_R(t)$ and the Loschmidt echo $\mathcal{M}_R(t)$ [31, 40]. The Loschmidt echo is a measure of the irreversibility suffered by the system during its evolution and generated by differences between forward and backward dynamics [32, 41–45]. In contrast, the fidelity quantifies the deviation of the dynamics of a state induced by a perturbation. In

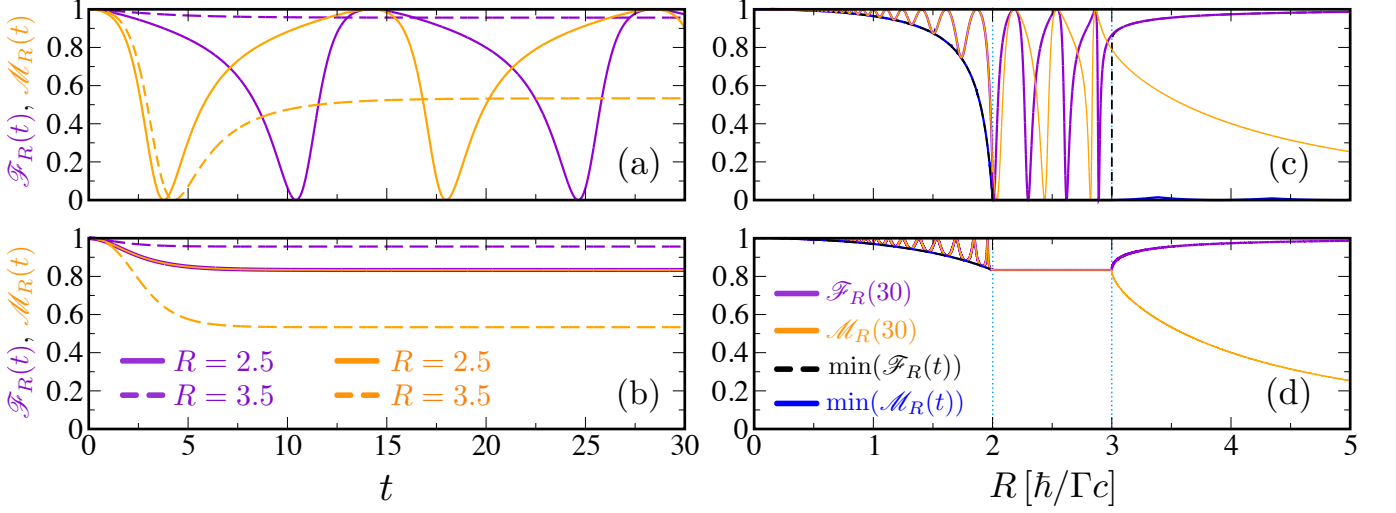


Figure 4. *Quench dynamics.* Fidelity $\mathcal{F}_R(t)$ (purple) and Loschmidt echo $\mathcal{M}_R(t)$ (orange) as a function of time (a)-(b) and as a function of the radius R (c)-(d) at $t = 30$ for two different mass quenches: (a) and (c) $\Gamma_i = 1/2$ and $\Gamma_f = 1/3$; (b) and (d) $\Gamma_i = 1/3$ and $\Gamma_f = 1/2$. For all cases we choose as the initial state the $|\psi_0\rangle = |\phi_{\Gamma_1,R}^{(n,m,\lambda)}\rangle$, the lowest pLL with $(n,m,\lambda) = (0, 1/2, 1)$ for the Hamiltonian \hat{H}_{Γ_i} .

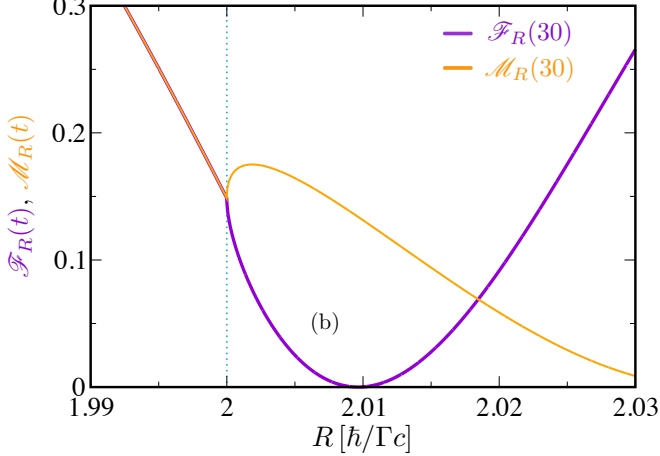


Figure 5. *Quench dynamics close to an EP.* Zoom of Fig.(4)c for the fidelity $\mathcal{F}_R(t)$ (purple) and Loschmidt echo $\mathcal{M}_R(t)$ (orange) as a function of radius R at $t = 30$ for the mass quench with $\Gamma_i = 1/2$ and $\Gamma_f = 1/3$ close to an exceptional radius $R = 2$. For $R < 2$, $\mathcal{F}_R(t) = \mathcal{M}_R(t)$. At $R = 2$ they bifurcate and assume different values.

NH systems, these perturbative effects are strongly increased in the proximity of the exceptional points [28]. We consider the case where the initial state, $|\psi_0\rangle = |\phi_{\Gamma_1,R}^{(n,m,\lambda)}\rangle$, is an eigenstate of \hat{H}_{Γ_1} , the case of a generic state can be obtained by an immediate generalization of this formalism. To simplify the notation used here, we omit the indexes n and m . With this choice, the eigenvector is written as $|\phi_{\Gamma_1,R}^{(\lambda)}\rangle$, where the upper index is related to the eigenvalue signal. The Loschmidt echo is defined as [31]

$$\mathcal{M}_R(t) = \frac{|\langle \psi_0 | \psi_f(t) \rangle|^2}{\langle \psi_0 | \psi_0 \rangle \langle \psi_f(t) | \psi_f(t) \rangle}. \quad (12)$$

The initial state is propagated forward in time with the Hamiltonian \hat{H}_{Γ_1} and then time reversed and propagated backward in time with \hat{H}_{Γ_2} to obtain $|\psi_f(t)\rangle$. Exploiting the orthogonality relations among the eigenstates of the Dirac Hamiltonian for different masses $\Gamma_{1,2}$ (see Appendix B) the expression of the time-evolved state can be greatly simplified

$$|\psi_f(t)\rangle = \sum_{\tilde{\lambda}=\pm} e^{\frac{i}{\hbar} [E_{\Gamma_2,R}^{(\tilde{\lambda})} - E_{\Gamma_1,R}^{(\tilde{\lambda})}] t} |\psi_{\Gamma_2,R}^{(\tilde{\lambda})}\rangle \times \langle \chi_{\Gamma_2,R}^{(\tilde{\lambda})} | \phi_{\Gamma_1,R}^{(\lambda)} \rangle. \quad (13)$$

Similarly, we compute the *time-dependent* fidelity $\mathcal{F}_R\{|\psi_1^{(\lambda)}(t)\rangle, |\psi_2^{(\lambda)}(t)\rangle\}$ defined in Eq.(9) between the time-evolved initial state $|\phi_{\Gamma_1,R}^{(\lambda)}\rangle$ under \hat{H}_{Γ_1} , i.e

$$|\psi_1^{(\lambda)}(t)\rangle = e^{-i\frac{t}{\hbar} E_{\Gamma_1,R}^{(\lambda)}} |\phi_{\Gamma_1,R}^{(\lambda)}\rangle, \quad (14)$$

and \hat{H}_{Γ_2} , i.e.

$$|\psi_2^{(\lambda)}(t)\rangle = \sum_{\ell=\pm} e^{-i\frac{t}{\hbar} E_{\Gamma_2,R}^{(\lambda)}} |\psi_{\Gamma_2,R}^{(\ell)}\rangle \langle \chi_{\Gamma_2,R}^{(\ell)} | \phi_{\Gamma_1,R}^{(\lambda)} \rangle. \quad (15)$$

The Loschmidt echo and the fidelity evaluated on the eigenstates of Eq.(1) satisfy the relation $\mathcal{F}_R^{(\lambda)}(t) = \mathcal{M}_R^{(-\lambda)}(t)$ (see Appendix C). Also, similarly to the Hermitian case, $\mathcal{F}_R^{(\lambda)}(t) = \mathcal{M}_R^{(\lambda)}(t)$ in the TR-invariant phase, whereas they generally differ in the TR-broken phase. In Fig.(4) we plot the fidelity and the Loschmidt echo as a function of time and the radius R of the sphere for quenches with $\Gamma_i > \Gamma_f$ (figs.(a) and (c)) and $\Gamma_i < \Gamma_f$ (figs.(b) and (d)) with the initial state $|\phi_{\Gamma_1,R}^{(1)}\rangle$, with $(n = 0, m = 1/2)$. For both $\Gamma_{i,f}$ we find two critical radii $R^* = 2$ and $R^* = 3$ (blue dotted lines) at which

we observe singularities for $\min_{t \in [0, \infty]} \mathcal{F}_R(t)$ (black dashed lines) and $\min_{t \in [0, \infty]} \mathcal{M}_R(t)$ (blue line). For quenches within the TR-invariant region for both \hat{H}_{Γ_i} and \hat{H}_{Γ_f} , when $R < 2$, the fidelity and the Loschmidt echo coincides at all times, $\mathcal{F}_R(t) = \mathcal{M}_R(t)$, (c-d). When $2 < R < 3$ they are equivalent only when $\Gamma_i < \Gamma_f$ and it is independent of the radius, (b) and (d). At larger radii $R > 3$, $\mathcal{F}_R(t) > \mathcal{M}_R(t)$ for both quenches, (c) and (d). Notice that in this limit the small minimum value of the Loschmidt echo $\min_{t \in [0, \infty]} \mathcal{M}_R(t)$ in (c) is attained at intermediate times (dashed-orange curve in (a)), whereas in (d) it coincides with the asymptotic value $\mathcal{M}_R(\infty)$ (dashed-orange curve in (b)). In Fig.(4)b we observe that for large times $\mathcal{F}_R(t)$ and $\mathcal{M}_R(t)$ converge to a constant. When $\lambda = 1$, with $\Gamma_1 > \Omega_{nm}$, $\Gamma_2 > \Omega_{nm}$ we have asymptotically ($t \rightarrow \infty$)

$$\mathcal{F}_R(t \rightarrow \infty) = \frac{\left| c_{\Gamma_2, \Gamma_1, R}^{(1,1)} \right|^2}{a_{\Gamma_2, \Gamma_1, R}^{(1,1,1)} \langle \psi_{\Gamma_1, R}^{(1)} | \psi_{\Gamma_1, R}^{(1)} \rangle}, \quad (16)$$

$$\mathcal{M}_R(t \rightarrow \infty) = \frac{\left| c_{\Gamma_2, \Gamma_1, R}^{(-1,1)} \right|^2}{\langle \psi_{\Gamma_1, R}^{(1)} | \psi_{\Gamma_1, R}^{(1)} \rangle b_{\Gamma_2, \Gamma_1, R}^{(-1,-1,1)}}, \quad (17)$$

where we introduced the constants

$$a_{\Gamma_2, \Gamma_1, R}^{(q, \ell, \lambda)} = \langle \chi_{\Gamma_2, R}^{(q)} | \psi_{\Gamma_1, R}^{(\lambda)} \rangle^* \langle \psi_{\Gamma_2, R}^{(q)} | \psi_{\Gamma_2, R}^{(\ell)} \rangle \langle \chi_{\Gamma_2, R}^{(\ell)} | \psi_{\Gamma_1, R}^{(\lambda)} \rangle, \quad (18)$$

$$b_{\Gamma_2, \Gamma_1, R}^{(q, \lambda, \ell)} = \langle \chi_{\Gamma_2, R}^{(q)} | \psi_{\Gamma_1, R}^{(\lambda)} \rangle^* \langle \chi_{\Gamma_2, R}^{(\ell)} | \psi_{\Gamma_1, R}^{(\lambda)} \rangle, \quad (19)$$

$$c_{\Gamma_2, \Gamma_1, R}^{(\ell, \lambda)} = \langle \chi_{\Gamma_2, R}^{(\ell)} | \psi_{\Gamma_1, R}^{(\lambda)} \rangle^* \langle \psi_{\Gamma_2, R}^{(\ell)} | \psi_{\Gamma_1, R}^{(\lambda)} \rangle. \quad (20)$$

In Fig.(5) we zoom on the region around the EP at $R = 2$ with $\Gamma_i = 1/2$ and $\Gamma_f = 1/3$, where the fidelity and the Loschmidt echo display a singularity and a bifurcation that display where the phase transition occurs.

IV. CONCLUSIONS

In this work we studied the influence of geometry in a prototypical problem of a Dirac particle moving on the surface of a sphere with an imaginary mass. From the analysis of the spectrum, we found an infinite sequence of EPs arising from PLLs in the presence of an imaginary mass. The NH magnetization and fidelity susceptibilities reveal phase transitions in correspondence of the EPs from TR-invariant to TR-broken phases. Finally, we investigated the quench dynamics through the Loschmidt echo and the fidelity and find singular behavior of these quantities at the EPs. Our work paves the way to study and analyze curvature-dependent NH phases where the curved background can be experimentally realized in synthetic systems [122–124]. Promising platforms to implement our model are the recent realizations of fullerene in a macroscopic-size superconducting resonator [80] and of Dirac surface states in topological nanoparticles [81, 82]. Several branches of future investigation can be anticipated, such as the influence of hyperbolic geometry [123] and the introduction of topological defects [125] in NH phases.

ACKNOWLEDGMENTS

We thank A. Lourenço and R. Arouca for useful discussions, and J. K. Pachos for valuable comments on the manuscript. This study was financed in part by the Coordenação de Aperfeiçoamento de Pessoal de Nível Superior – Brasil (CAPES) – Finance Code 001. T.M. acknowledges CNPq for support through Bolsa de produtividade em Pesquisa n.311079/2015-6. This work was supported by the Serrapilheira Institute (grant number Serra-1812-27802), CAPES-NUFFIC project number 88887.156521/2017-00.

APPENDIX

in this Appendix we present some technical details on the derivation of the spectrum of the Dirac Hamiltonian with imaginary mass, the biorthogonal basis, and the relevant scalar products for the dynamics.

Appendix A: Spectrum of the Dirac Hamiltonian with imaginary mass

In this Appendix we briefly review the calculations to the eigenvalue problem for Dirac hamiltonian with imaginary mass on the sphere. First we shall derive the differential equation for the spinor components, find the eigenvalues and the general form of the solutions.

The eigenfunctions of \hat{H}_{Γ} are two-component spinors that satisfy the eigenvalue equation given by $\hat{H}_{\Gamma} \phi_{\Gamma, R}^{(m)}(\theta, \varphi) = E_{\Gamma, R}^{(m)} \phi_{\Gamma, R}^{(m)}(\theta, \varphi)$, where

$$\phi_{\Gamma, R}^{(m)}(\theta, \varphi) = \frac{e^{im\varphi}}{\sqrt{4\pi}} \begin{pmatrix} \alpha_{\Gamma, R}^{(m)}(\theta) \\ \beta_{\Gamma, R}^{(m)}(\theta) \end{pmatrix}, \quad (A1)$$

with $m = \pm \frac{1}{2}, \pm \frac{3}{2}, \dots$

Now, we have

$$\frac{\hbar c}{R} \hat{h}^- \left[e^{im\varphi} \beta_{\Gamma, R}^{(m)}(\theta) \right] = \left(E_{\Gamma, R}^{(m)} + i c^2 \Gamma \right) e^{im\varphi} \alpha_{\Gamma, R}^{(m)}(\theta); \quad (A2a)$$

$$\frac{\hbar c}{R} \hat{h}^+ \left[e^{im\varphi} \alpha_{\Gamma, R}^{(m)}(\theta) \right] = \left(E_{\Gamma, R}^{(m)} - i c^2 \Gamma \right) e^{im\varphi} \beta_{\Gamma, R}^{(m)}(\theta). \quad (A2b)$$

These two equations combine, after a change of variables $\zeta = \cos \theta$, to give [70, 71]

$$\left[\frac{d}{d\zeta} (1 - \zeta^2) \frac{d}{d\zeta} - \frac{m^2 - \sigma_z m \zeta + 1/4}{1 - \zeta^2} + \Omega^2 - \frac{1}{4} \right] \begin{pmatrix} \alpha_{\Gamma, R}^{(m)}(\zeta) \\ \beta_{\Gamma, R}^{(m)}(\zeta) \end{pmatrix} = 0. \quad (A3)$$

with

$$\Omega^2 = \frac{R^2}{\hbar^2 c^2} (E_m^2 + \Gamma^2 c^4). \quad (A4)$$

Changing the variables as

$$\begin{pmatrix} \alpha_m(\zeta) \\ \beta_m(\zeta) \end{pmatrix} = \begin{pmatrix} (1-\zeta)^{\frac{1}{2}|m-\frac{1}{2}|} (1+\zeta)^{\frac{1}{2}|m+\frac{1}{2}|} \xi_m(\zeta) \\ (1-\zeta)^{\frac{1}{2}|m+\frac{1}{2}|} (1+\zeta)^{\frac{1}{2}|m-\frac{1}{2}|} \eta_m(\zeta) \end{pmatrix}, \quad (\text{A5})$$

one can verify

$$\left\{ (1-\zeta^2) \frac{d^2}{d\zeta^2} + \left[\frac{m}{|m|} \sigma_3 - (2|m|+2)\zeta \right] \frac{d}{d\zeta} + \right. \\ \left. - |m|(|m|+1) + \left(\Omega_{nm}^2 - \frac{1}{4} \right) \right\} \begin{pmatrix} \xi_m(\zeta) \\ \eta_m(\zeta) \end{pmatrix} = 0. \quad (\text{A6})$$

For square integrable solutions [70] on the interval $x \in [-1, 1]$, we need that $\Omega_{nm}^2 = (n+|m|+\frac{1}{2})^2$, whith non-negative integer $n \geq 0$.

Now, $\xi_{nm}(\zeta)$ and $\eta_{nm}(\zeta)$ are expressed in terms of the n -th order Jacobi polynomial as

$$\begin{pmatrix} \xi_{nm}(\zeta) \\ \eta_{nm}(\zeta) \end{pmatrix} = \begin{pmatrix} c_{nm}^\alpha P_n^{(|m-1/2|, |m+1/2|)}(\zeta) \\ c_{nm}^\beta P_n^{(|m+1/2|, |m-1/2|)}(\zeta) \end{pmatrix}. \quad (\text{A7})$$

From Eqs.(A2) we find a condition for the coefficients

$$c_{\Gamma,R}^{\beta(n,m,\lambda)} = -\text{sgn}[m] \frac{\left[E_{\Gamma,R}^{(n,m,\lambda)} + i\Gamma c^2 \right]}{\frac{\hbar c}{R} \Omega_{nm}} c_{\Gamma,R}^{\alpha(n,m,\lambda)}, \quad (\text{A8a})$$

$$c_{\Gamma,R}^{\alpha(n,m,\lambda)} = -\text{sgn}[m] \frac{\left[E_{\Gamma,R}^{(n,m,\lambda)} - i\Gamma c^2 \right]}{\frac{\hbar c}{R} \Omega_{nm}} c_{\Gamma,R}^{\beta(n,m,\lambda)}. \quad (\text{A8b})$$

The absolute values of the constants can be found from the normalization conditions,

$$\int_0^{2\pi} \int_{-1}^1 \left[\phi_{nm}^{(\lambda)}(\zeta, \varphi) \right]^\dagger \phi_{nm}^{(\lambda)}(\theta, \varphi) R^2 d\zeta d\varphi = 1. \quad (\text{A9})$$

Therefore,

$$\left| c_{\Gamma,R}^{\alpha(n,m,\lambda)} \right| = \sqrt{\frac{\frac{\hbar^2 c^2 \Omega_{nm}^2 n! (n+2|m|)!}{R^2 2^{2|m|-1} \Gamma(\Omega_{nm})^2 R^2}}{\frac{\hbar^2 c^2}{R^2} \Omega_{nm}^2 + \left| E_{\Gamma,R}^{(n,m,\lambda)} + i\Gamma c^2 \right|^2}}. \quad (\text{A10})$$

The Eq. (A1) becomes

$$\phi_{\Gamma,R}^{(n,m,\lambda)}(\zeta, \varphi) = c_{\Gamma,R}^{\alpha(n,m,\lambda)} a_{\Gamma,R}^{(n,m,\lambda)} \times \\ \times \frac{e^{im\varphi}}{\sqrt{4\pi}} \begin{pmatrix} A_{nm}(\zeta) \\ -\frac{E_{\Gamma,R}^{(n,m,\lambda)} + i\Gamma c^2}{\text{sgn}[m] \frac{\hbar c}{R} \Omega_{nm}} B_{nm}(\zeta) \end{pmatrix}, \quad (\text{A11})$$

where

$$A_{nm}(\zeta) = \sqrt{1-\zeta^{|m-\frac{1}{2}|}} \sqrt{1+\zeta^{|m+\frac{1}{2}|}} P_n^{(|m-\frac{1}{2}|, |m+\frac{1}{2}|)}(\zeta), \quad (\text{A12a})$$

$$B_{nm}(\zeta) = \sqrt{1-\zeta^{|m+\frac{1}{2}|}} \sqrt{1+\zeta^{|m-\frac{1}{2}|}} P_n^{(|m+\frac{1}{2}|, |m-\frac{1}{2}|)}(\zeta), \quad (\text{A12b})$$

and $a_{\Gamma,R}^{(n,m,\lambda)} = \sqrt{E_{\Gamma,R}^{(n,m,\lambda)} + i\Gamma c^2} / \left| \sqrt{E_{\Gamma,R}^{(n,m,\lambda)} + i\Gamma c^2} \right|$. The

introduction of the term $a_{\Gamma,R}^{(n,m,\lambda)}$ is useful for considerations on the TR symmetry.

Appendix B: Details on the biorthogonal basis: eigenvectors and scalar products

In this Appendix we show the eigenvectors of \hat{H}_Γ and \hat{H}_Γ^\dagger and the scalar product between them with different parameters at fixed radius. These relations we will be useful to study the quantum quenches. To obtain these quantities, we follow the same steps of Appendix B using Eq.(6) to impose the correct normalization.

The eigenvectors of the Hamiltonians \hat{H}_Γ and \hat{H}_Γ^\dagger are given by, respectively,

$$\psi_{\Gamma,R}^{(n,m,\lambda)} = f_{\Gamma,R}^{(n,m,\lambda)} \frac{e^{im\varphi}}{\sqrt{4\pi}} \begin{pmatrix} A_{nm}(\zeta) \\ -\frac{[E_{\Gamma,R}^{(n,m,\lambda)} + i\Gamma c^2]}{\text{sgn}[m] \frac{\hbar c}{R} \Omega_{nm}} B_{nm}(\zeta) \end{pmatrix}, \quad (\text{B1})$$

$$\chi_{\Gamma,R}^{(n,m,\lambda)} = f_{\Gamma,R}^{(n,m,\lambda)*} \frac{e^{im\varphi}}{\sqrt{4\pi}} \begin{pmatrix} A_{nm}(\zeta) \\ -\frac{[\Xi_{\Gamma,R}^{(n,m,\lambda)} - i\Gamma c^2]}{\text{sgn}[m] \frac{\hbar c}{R} \Omega_{nm}} B_{nm}(\zeta) \end{pmatrix}, \quad (\text{B2})$$

where

$$f_{\Gamma,R}^{(n,m,\lambda)} = \sqrt{\frac{n! \Gamma(n+2|m|+1) \frac{\hbar^2 c^2}{R^2} \Omega_{nm}^2}{\frac{2^{2|m|-1} \Gamma(\Omega_{nm})^2 R^2}{\frac{\hbar^2 c^2}{R^2} \Omega_{nm}^2 + [E_{\Gamma,R}^{(n,m,\lambda)} + i\Gamma c^2]^2}}}. \quad (\text{B3})$$

The relevant scalar products for different values of Γ and λ for the states of Eqs.(B1) and (B2) are given by

$$\langle \chi_{\Gamma_1,R}^{(\lambda_1)} | \psi_{\Gamma_2,R}^{(\lambda_2)} \rangle = \frac{f_{\Gamma_1,R}^{(n,m,\lambda_1)} f_{\Gamma_2,R}^{(n,m,\lambda_2)} R^2 2^{2|m|-1} \Gamma(\Omega_{nm})^2}{(\hbar^2 c^2 / R^2) \Omega_{nm}^2 n! \Gamma(n+2|m|+1)} \times \\ \times \left(\frac{\hbar^2 c^2}{R^2} \Omega_{nm}^2 + [E_{\Gamma_1,R}^{(n,m,\lambda_1)} + i\Gamma_1 c^2] [E_{\Gamma_2,R}^{(n,m,\lambda_2)} + i\Gamma_2 c^2] \right) \quad (\text{B4})$$

and

$$\langle \psi_{\Gamma_1,R}^{(\lambda_1)} | \psi_{\Gamma_2,R}^{(\lambda_2)} \rangle = \frac{f_{\Gamma_1,R}^{(n,m,\lambda_1)} f_{\Gamma_2,R}^{(n,m,\lambda_2)} R^2 2^{2|m|-1} \Gamma(\Omega_{nm})^2}{(\hbar^2 c^2 / R^2) \Omega_{nm}^2 n! \Gamma(n+2|m|+1)} \times \\ \times \left(\frac{\hbar^2 c^2}{R^2} \Omega_{nm}^2 + [E_{\Gamma_1,R}^{(n,m,\lambda_1)} + i\Gamma_1 c^2]^* [E_{\Gamma_2,R}^{(n,m,\lambda_2)} + i\Gamma_2 c^2] \right). \quad (\text{B5})$$

Appendix C: Dynamics induced by a mass quench: Fidelity and Loschmidt echo

In this Appendix we briefly review the calculations of the Loschmidt echo and the fidelity. These quantities measure the sensitivity to perturbations of the backward evolution.

Given the state $|\psi_{\Gamma_1,R}^{(\lambda)}\rangle$ at $t=0$, if $\hat{H}_{\Gamma_1,2}$ is independent of time, then its time evolution is

$$|\psi_{\Gamma_1}^{(\lambda)}(t)\rangle = e^{-i\frac{t}{\hbar} \hat{H}_{\Gamma_1,R}^{(\lambda)}} |\psi_{\Gamma_1,R}^{(\lambda)}\rangle. \quad (\text{C1})$$

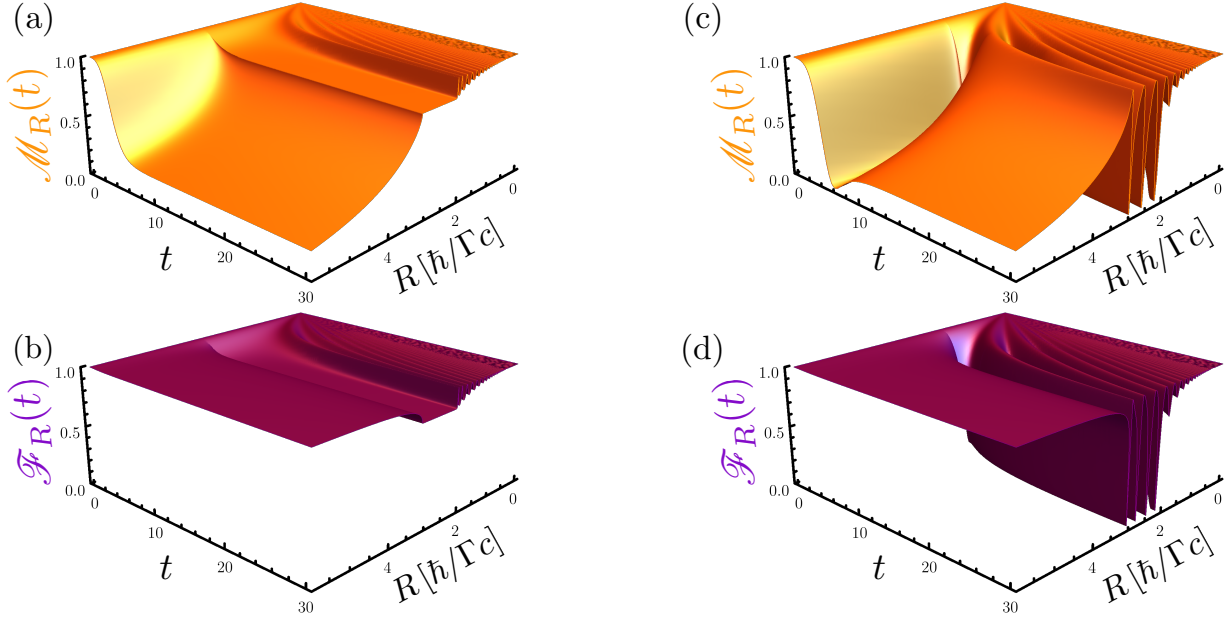


Figure 6. Three-dimensional plot of the fidelity $\mathcal{F}_R(t)$ (orange) and Loschmidt echo $\mathcal{M}_R(t)$ (purple) in function of the sphere radius R and time t for the mass quenches: (a) and (b) $\Gamma_i = 1/3$ and $\Gamma_f = 1/2$. (c) and (d) $\Gamma_i = 1/2$ and $\Gamma_f = 1/3$. For all cases we choose as the initial state the $|\psi_0\rangle = |\phi_{\Gamma_1,R}^{(n,m,\lambda)}\rangle$, the lowest pLL with $(n,m,\lambda) = (0, 1/2, 1)$ for the Hamiltonian \hat{H}_{Γ_1}

In terms of the biorthogonal basis we can write

$$|\psi_{\Gamma_2}^{(\lambda)}(t)\rangle = \sum_{\ell} e^{-i\frac{t}{\hbar}E_{\Gamma_2,R}^{(\lambda)}} |\psi_{\Gamma_2,R}^{(\ell)}\rangle \langle \chi_{\Gamma_2,R}^{(\ell)} | \psi_{\Gamma_1,R}^{(\lambda)} \rangle. \quad (\text{C2})$$

Computing the corresponding bras as

$$\langle \psi_{\Gamma_1}^{(\lambda)}(t) | = e^{i\frac{t}{\hbar}E_{\Gamma_1,R}^{(\lambda)*}} \langle \psi_{\Gamma_1,R}^{(\lambda)}, \quad (\text{C3})$$

$$\langle \psi_{\Gamma_2}^{(\lambda)}(t) | = \sum_{\ell} e^{i\frac{t}{\hbar}E_{\Gamma_2,R}^{(\ell)*}} \langle \chi_{\Gamma_2,R}^{(\ell)} | \phi_{\Gamma_1,R}^{(\lambda)} \rangle^* \langle \psi_{\Gamma_2,R}^{(\ell)} |, \quad (\text{C4})$$

we define the fidelity $\mathcal{F}_R(t)$ as

$$\mathcal{F}_R(t) = \frac{\left| \langle \psi_{\Gamma_1}^{(\lambda)}(t) | \psi_{\Gamma_2}^{(\lambda)}(t) \rangle \right|^2}{\langle \psi_{\Gamma_1}^{(\lambda)}(t) | \psi_{\Gamma_1}^{(\lambda)}(t) \rangle \langle \psi_{\Gamma_2}^{(\lambda)}(t) | \psi_{\Gamma_2}^{(\lambda)}(t) \rangle}, \quad (\text{C5})$$

with

$$\langle \psi_{\Gamma_1}^{(\lambda)}(t) | \psi_{\Gamma_2}^{(\lambda)}(t) \rangle = \sum_{\ell} e^{i\frac{t}{\hbar}[E_{\Gamma_1,R}^{(\lambda)*} - E_{\Gamma_2,R}^{(\ell)}]} \times \langle \psi_{\Gamma_1,R}^{(\lambda)} | \psi_{\Gamma_2,R}^{(\ell)} \rangle \langle \chi_{\Gamma_2,R}^{(\ell)} | \psi_{\Gamma_1,R}^{(\lambda)} \rangle, \quad (\text{C6})$$

$$\langle \psi_{\Gamma_2}^{(\lambda)}(t) | \psi_{\Gamma_1}^{(\lambda)}(t) \rangle = \sum_q \sum_{\ell} e^{i\frac{t}{\hbar}[E_{\Gamma_2,R}^{(q)*} - E_{\Gamma_1,R}^{(\ell)}]} \times \langle \chi_{\Gamma_2,R}^{(q)} | \psi_{\Gamma_1,R}^{(\lambda)} \rangle^* \langle \psi_{\Gamma_2,R}^{(q)} | \psi_{\Gamma_2,R}^{(\ell)} \rangle \langle \chi_{\Gamma_2,R}^{(\ell)} | \psi_{\Gamma_1,R}^{(\lambda)} \rangle, \quad (\text{C7})$$

$$\langle \psi_{\Gamma_1}^{(\lambda)}(t) | \psi_{\Gamma_1}^{(\lambda)}(t) \rangle = e^{i\frac{t}{\hbar}[E_{\Gamma_1}^{(\lambda)*} - E_{\Gamma_1}^{(\lambda)}]} \langle \psi_{\Gamma_1,R}^{(\lambda)} | \psi_{\Gamma_1,R}^{(\lambda)} \rangle. \quad (\text{C8})$$

Note that we use the definition of $\psi_{\Gamma_2,R}^{(\ell)}$ normalized according to the biorthogonal basis, i.e., Eq. (B1).

Let us consider an initial state $|\psi_0^{(\lambda)}\rangle$ at time $t = 0$ an eigenstate of the \hat{H}_{Γ_1} , i.e., $|\psi_{\Gamma_1,R}^{(\lambda)}\rangle$. We define the evolution of this state as $|\psi_f^{(\lambda)}\rangle = e^{i\frac{t}{\hbar}H_{\Gamma_2}} e^{-i\frac{t}{\hbar}H_{\Gamma_1}} |\psi_{\Gamma_1}^{(\lambda)}\rangle$. The Loschmidt echo $\mathcal{M}(t)$ is defined as

$$\mathcal{M}_R(t) = \frac{\left| \langle \psi_0^{(\lambda)} | \psi_f^{(\lambda)} \rangle \right|^2}{\langle \psi_0^{(\lambda)} | \psi_0^{(\lambda)} \rangle \langle \psi_f^{(\lambda)} | \psi_f^{(\lambda)} \rangle}, \quad (\text{C9})$$

with

$$\langle \psi_0^{(\lambda)} | \psi_f^{(\lambda)} \rangle = e^{-i\frac{t}{\hbar}E_{\Gamma_1}^{(\lambda)}} \sum_{\ell} e^{i\frac{t}{\hbar}E_{\Gamma_2}^{(\ell)}} \langle \psi_{\Gamma_1}^{(\lambda)} | \psi_{\Gamma_2}^{(\ell)} \rangle \langle \chi_{\Gamma_2}^{(\ell)} | \psi_{\Gamma_1}^{(\lambda)} \rangle, \quad (\text{C10})$$

$$\langle \psi_f^{(\lambda)} | \psi_f^{(\lambda)} \rangle = e^{i\frac{t}{\hbar}[E_{\Gamma_1}^{(\lambda)*} - E_{\Gamma_1}^{(\lambda)}]} \sum_q \sum_{\ell} e^{i\frac{t}{\hbar}[E_{\Gamma_2}^{(\ell)} - E_{\Gamma_2}^{(q)*}]} \times \langle \chi_{\Gamma_2}^{(q)} | \psi_{\Gamma_1}^{(\lambda)} \rangle^* \langle \psi_{\Gamma_2}^{(q)} | \psi_{\Gamma_2}^{(\ell)} \rangle \langle \chi_{\Gamma_2}^{(\ell)} | \psi_{\Gamma_1}^{(\lambda)} \rangle, \quad (\text{C11})$$

$$\langle \psi_0^{(\lambda)} | \psi_0^{(\lambda)} \rangle = \langle \psi_{\Gamma_1,R}^{(\lambda)} | \psi_{\Gamma_1,R}^{(\lambda)} \rangle. \quad (\text{C12})$$

In Fig.(6) we show the three-dimensional plot of $\mathcal{F}_R(t)$ and $\mathcal{M}_R(t)$ for the two quenches with different values of Γ .

* ygpara@fisica.ufn.br

† giandomenico.palumbo@gmail.com

‡ macri@fisica.ufn.br

[1] K. Esaki, M. Sato, K. Hasebe, and M. Kohmoto, Phys. Rev. B **84**, 205128 (2011).

- [2] K. Kawabata, K. Shiozaki, M. Ueda, and M. Sato, *Phys. Rev. X* **9**, 041015 (2019).
- [3] Z. Gong, Y. Ashida, K. Kawabata, K. Takasan, S. Higashikawa, and M. Ueda, *Phys. Rev. X* **8**, 031079 (2018).
- [4] E. J. Bergholtz, J. C. Budich, and F. K. Kunst, *arXiv:1912.10048* (2019).
- [5] V. M. Martinez Alvarez, J. E. Barrios Vargas, M. Berdakin, and L. E. F. Foa Torres, *Eur. Phys. J. Special Topics* **227**, 1295 (2018).
- [6] H. Zhou and J. Y. Lee, *Phys. Rev. B* **99**, 235112 (2019).
- [7] H. Shen, B. Zhen, and L. Fu, *Phys. Rev. Lett.* **120**, 146402 (2018).
- [8] J. M. Zeuner, M. C. Rechtsman, Y. Plotnik, Y. Lumer, S. Nolte, M. S. Rudner, M. Segev, and A. Szameit, *Phys. Rev. Lett.* **115**, 040402 (2015).
- [9] K. Yamamoto, M. Nakagawa, K. Adachi, K. Takasan, M. Ueda, and N. Kawakami, *Phys. Rev. Lett.* **123**, 123601 (2019).
- [10] T. Yoshida, K. Kudo, and Y. Hatsugai, *Scientific Reports* **9**, 10.1038/s41598-019-53253-8 (2019).
- [11] N. Okuma, K. Kawabata, K. Shiozaki, and M. Sato, *Phys. Rev. Lett.* **124**, 086801 (2020).
- [12] C. H. Lee and R. Thomale, *Phys. Rev. B* **99**, 201103 (2019).
- [13] S. Longhi, *Phys. Rev. Research* **1**, 023013 (2019).
- [14] Y. Yi and Z. Yang, *Phys. Rev. Lett.* **125**, 186802 (2020).
- [15] F. K. Kunst, E. Edvardsson, J. C. Budich, and E. J. Bergholtz, *Phys. Rev. Lett.* **121**, 026808 (2018).
- [16] S. Yao, F. Song, and Z. Wang, *Phys. Rev. Lett.* **121**, 136802 (2018).
- [17] H. Wang, J. Ruan, and H. Zhang, *Phys. Rev. B* **99**, 075130 (2019).
- [18] D. S. Borgnia, A. J. Kruchkov, and R.-J. Slager, *Phys. Rev. Lett.* **124**, 056802 (2020).
- [19] K.-I. Imura and Y. Takane, *Phys. Rev. B* **100**, 165430 (2019).
- [20] C. M. Bender and S. Boettcher, *Phys. Rev. Lett.* **80**, 5243 (1998).
- [21] W. B. Rui, M. M. Hirschmann, and A. P. Schnyder, *Phys. Rev. B* **100**, 245116 (2019).
- [22] J. C. Budich, J. Carlström, F. K. Kunst, and E. J. Bergholtz, *Phys. Rev. B* **99**, 041406 (2019).
- [23] K. Kawabata, T. Bessho, and M. Sato, *Phys. Rev. Lett.* **123**, 066405 (2019).
- [24] T. Yoshida, R. Peters, N. Kawakami, and Y. Hatsugai, *Phys. Rev. B* **99**, 121101 (2019).
- [25] L. Zhou, Q.-h. Wang, H. Wang, and J. Gong, *Phys. Rev. A* **98**, 022129 (2018).
- [26] R. Arouca, C. H. Lee, and C. Morais Smith, *arXiv:2009.03541* (2020).
- [27] D. Leykam, K. Y. Bliokh, C. Huang, Y. D. Chong, and F. Nori, *Phys. Rev. Lett.* **118**, 040401 (2017).
- [28] Y.-C. Tzeng, C.-Y. Ju, G.-Y. Chen, and W.-M. Huang, *Phys. Rev. Research* **3**, 013015 (2021).
- [29] G. Sun and S.-P. Kou, *arXiv:2009.11183* (2020).
- [30] N. Matsumoto, K. Kawabata, Y. Ashida, S. Furukawa, and M. Ueda, *arXiv:1912.09045* (2019).
- [31] S. Longhi, *Annalen der Physik* **531**, 1900054 (2019).
- [32] R. Jafari and H. Johannesson, *Phys. Rev. Lett.* **118**, 015701 (2017).
- [33] T. Gorin, T. Prosen, T. H. Seligman, and M. Žnidarič, *Physics Reports* **435**, 33 (2006).
- [34] S. T. Amin, B. Mera, C. Vlachou, N. Paunković, and V. R. Vieira, *Phys. Rev. B* **98**, 245141 (2018).
- [35] C. De Grandi, V. Gritsev, and A. Polkovnikov, *Phys. Rev. B* **81**, 012303 (2010).
- [36] P. Zanardi, P. Giorda, and M. Cozzini, *Phys. Rev. Lett.* **99**, 100603 (2007).
- [37] N. Paunković and V. Rocha Vieira, *Phys. Rev. E* **77**, 011129 (2008).
- [38] A. F. Albuquerque, F. Alet, C. Sire, and S. Capponi, *Phys. Rev. B* **81**, 064418 (2010).
- [39] S.-J. Gu, H.-M. Kwok, W.-Q. Ning, and H.-Q. Lin, *Phys. Rev. B* **77**, 245109 (2008).
- [40] T. Macrì, A. Smerzi, and L. Pezzè, *Phys. Rev. A* **94**, 010102 (2016).
- [41] A. Goussev, R. A. Jalabert, H. M. Pastawski, and D. A. Wisniacki, *Philosophical Transactions of the Royal Society A: Mathematical, Physical and Engineering Sciences* **374**, 20150383 (2016).
- [42] H. T. Quan, Z. Song, X. F. Liu, P. Zanardi, and C. P. Sun, *Phys. Rev. Lett.* **96**, 140604 (2006).
- [43] L. Campos Venuti and P. Zanardi, *Phys. Rev. A* **81**, 022113 (2010).
- [44] F. Pollmann, S. Mukerjee, A. G. Green, and J. E. Moore, *Phys. Rev. E* **81**, 020101 (2010).
- [45] B. Mera, C. Vlachou, N. Paunković, V. R. Vieira, and O. Viyuela, *Phys. Rev. B* **97**, 094110 (2018).
- [46] D. P. Pires, A. Smerzi, and T. Macrì, *Phys. Rev. A* **102**, 012429 (2020).
- [47] K. Macieszczak, E. Levi, T. Macrì, I. Lesanovsky, and J. P. Garrahan, *Phys. Rev. A* **99**, 052354 (2019).
- [48] F. de Juan, A. Cortijo, and M. A. H. Vozmediano, *Phys. Rev. B* **76**, 165409 (2007).
- [49] O. Boada, A. Celi, J. I. Latorre, and M. Lewenstein, *New Journal of Physics* **13**, 035002 (2011).
- [50] S. Ryu, J. E. Moore, and A. W. W. Ludwig, *Phys. Rev. B* **85**, 045104 (2012).
- [51] M. Stone, *Phys. Rev. B* **85**, 184503 (2012).
- [52] T. L. Hughes, R. G. Leigh, and O. Parrikar, *Phys. Rev. D* **88**, 025040 (2013).
- [53] G. Palumbo, R. Catenacci, and A. Marzuoli, *Int. J. Mod. Phys. B* **28**, 1350193 (2014).
- [54] A. Iorio and G. Lambiase, *Phys. Rev. D* **90**, 025006 (2014).
- [55] G. Palumbo and J. K. Pachos, *Ann. Phys.* **372**, 175 (2016).
- [56] C. Koke, C. Noh, and D. G. Angelakis, *Ann. Phys.* **374**, 162 (2016).
- [57] K. Landsteiner, Y. Liu, and Y.-W. Sun, *Phys. Rev. Lett.* **117**, 081604 (2016).
- [58] G. Palumbo, *Ann. Phys.* **386**, 15 (2017).
- [59] A. Celi, *The European Physical Journal Special Topics* **226**, 2729 (2017).
- [60] A. Westström and T. Ojanen, *Phys. Rev. X* **7**, 041026 (2017).
- [61] T. Kvorning, T. H. Hansson, A. Quelle, and C. M. Smith, *Phys. Rev. Lett.* **120**, 217002 (2018).
- [62] P. Maraner, J. K. Pachos, and G. Palumbo, *Scientific Reports* **9**, 10.1038/s41598-019-53771-5 (2019).
- [63] J. Nissinen, *Phys. Rev. Lett.* **124**, 117002 (2020).
- [64] J. Nissinen and G. E. Volovik, *Phys. Rev. Research* **2**, 033269 (2020).
- [65] A. Farjami, M. D. Horner, C. N. Self, Z. Papić, and J. K. Pachos, *Phys. Rev. B* **101**, 245116 (2020).
- [66] T. Inagaki and K. Ishikawa, *Phys. Rev. D* **56**, 5097 (1997).
- [67] P. Gentile, M. Cuoco, and C. Ortix, *Phys. Rev. Lett.* **115**, 256801 (2015).
- [68] E. V. Castro, A. Flachi, P. Ribeiro, and V. Vitagliano, *Phys. Rev. Lett.* **121**, 221601 (2018).
- [69] Z. B. Siu, J.-Y. Chang, S. G. Tan, M. B. A. Jalil, and C.-R. Chang, *Scientific Reports* **8**, 16497 (2018).
- [70] A. A. Abrikosov Jr., arXiv e-prints , hep-th/0212134 (2002),

- arXiv:hep-th/0212134 [hep-th].
- [71] A. A. Abrikosov Jr, *Quantum field theory under the influence of external conditions. Proceedings, 5th Workshop, Leipzig, Germany, September 10-14, 2001*, Int. J. Mod. Phys. **A17**, 885 (2002), arXiv:hep-th/0111084 [hep-th].
 - [72] D. V. Kolesnikov and V. A. Osipov, The European Physical Journal B **49**, 465 (2006).
 - [73] J. González, F. Guinea, and M. A. H. Vozmediano, Nuclear Physics B **406**, 771 (1993).
 - [74] M. Vozmediano, M. Katsnelson, and F. Guinea, Physics Reports **496**, 109 (2010).
 - [75] R. Pincak, Physics Letters A **340**, 267 (2005).
 - [76] J. K. Pachos, M. Stone, and K. Temme, Phys. Rev. Lett. **100**, 156806 (2008).
 - [77] Y. Takane and K.-I. Imura, Journal of the Physical Society of Japan **82**, 074712 (2013), <https://doi.org/10.7566/JPSJ.82.074712>.
 - [78] K.-I. Imura, Y. Yoshimura, Y. Takane, and T. Fukui, Phys. Rev. B **86**, 235119 (2012).
 - [79] D.-H. Lee, Phys. Rev. Lett. **103**, 196804 (2009).
 - [80] B. Dietz, T. Klaus, M. Miski-Oglu, A. Richter, M. Bischoff, L. von Smekal, and J. Wambach, Phys. Rev. Lett. **115**, 026801 (2015).
 - [81] G. Siroki, D. Lee, P. D. Haynes, and V. Giannini, Nature Communications **7**, 10.1038/ncomms12375 (2016).
 - [82] M. S. Rider, M. Sokolikova, S. M. Hanham, M. Navarro-Cía, P. D. Haynes, D. K. K. Lee, M. Daniele, M. C. Guidi, C. Mattevi, S. Lupi, and V. Giannini, Nanoscale **12**, 22817 (2020).
 - [83] A. Szameit, M. C. Rechtsman, O. Bahat-Treidel, and M. Segev, Phys. Rev. A **84**, 021806 (2011).
 - [84] Z.-Y. Ge, Y.-R. Zhang, T. Liu, S.-W. Li, H. Fan, and F. Nori, Phys. Rev. B **100**, 054105 (2019).
 - [85] X. Ni, D. Smirnova, A. Poddubny, D. Leykam, Y. Chong, and A. B. Khanikaev, Phys. Rev. B **98**, 165129 (2018).
 - [86] W. B. Rui, Y. X. Zhao, and A. P. Schnyder, Phys. Rev. B **99**, 241110 (2019).
 - [87] P. Xue, L. Xiao, D. Qu, K. Wang, H.-W. Li, J.-Y. Dai, B. Dora, M. Heyl, R. Moessner, and W. Yi, Non-hermitian kibble-zurek mechanism with tunable complexity in single-photon interferometry (2020), arXiv:2004.05928 [quant-ph].
 - [88] H. Schomerus and N. Y. Halpern, Phys. Rev. Lett. **110**, 013903 (2013).
 - [89] F. de Juan, J. L. Mañes, and M. A. H. Vozmediano, Phys. Rev. B **87**, 165131 (2013).
 - [90] D. I. Pikulin, A. Chen, and M. Franz, Phys. Rev. X **6**, 041021 (2016).
 - [91] S. Rachel, I. Göthel, D. P. Arovas, and M. Vojta, Phys. Rev. Lett. **117**, 266801 (2016).
 - [92] A. G. Grushin, J. W. F. Venderbos, A. Vishwanath, and R. Ilan, Phys. Rev. X **6**, 041046 (2016).
 - [93] G. Salerno, T. Ozawa, H. M. Price, and I. Carusotto, Phys. Rev. B **95**, 245418 (2017).
 - [94] Z.-M. Huang, B. Han, and M. Stone, Phys. Rev. B **101**, 125201 (2020).
 - [95] S. Laurila and J. Nissinen, Phys. Rev. B **102**, 235163 (2020).
 - [96] R. M. Wald, *General Relativity* (Chicago Univ. Pr., Chicago, USA, 1984).
 - [97] S. Weinberg, *Gravitation and Cosmology: Principles and Applications of the General Theory of Relativity* (John Wiley and Sons, New York, 1972).
 - [98] M. Pollock, Acta Phys. Polon. B **41**, 1827 (2010).
 - [99] P. Collas and D. Klein, *The Dirac Equation in Curved Space-time* (Springer International Publishing, 2019).
 - [100] M. Arminjon, International Journal of Theoretical Physics **54**, 2218 (2014).
 - [101] J. González, F. Guinea, and M. A. H. Vozmediano, Phys. Rev. Lett. **69**, 172 (1992).
 - [102] K. Yonaga, K. Hasebe, and N. Shibata, Phys. Rev. B **93**, 235122 (2016).
 - [103] W.-H. Hsiao, Phys. Rev. B **101**, 155310 (2020).
 - [104] T. Neupert, S. Rachel, R. Thomale, and M. Greiter, Phys. Rev. Lett. **115**, 017001 (2015).
 - [105] M. Greiter and R. Thomale, Annals of Physics **394**, 33 (2018).
 - [106] R. Ilan, A. G. Grushin, and D. I. Pikulin, Nature Reviews Physics **2**, 29 (2019).
 - [107] M. Arcinaga and M. R. Peterson, Phys. Rev. B **94**, 035105 (2016).
 - [108] P. Castro-Villarreal and R. Ruiz-Sánchez, Phys. Rev. B **95**, 125432 (2017).
 - [109] C. M. Bender and S. Boettcher, Phys. Rev. Lett. **80**, 5243 (1998).
 - [110] T. Kato, *Perturbation Theory for Linear Operators* (Springer Berlin Heidelberg, 1995).
 - [111] M. Greiter, Phys. Rev. B **83**, 115129 (2011).
 - [112] F. D. M. Haldane, Phys. Rev. Lett. **51**, 605 (1983).
 - [113] X. Huang and L. Parker, Phys. Rev. D **79**, 024020 (2009).
 - [114] R. Camporesi and A. Higuchi, Journal of Geometry and Physics **20**, 1 (1996).
 - [115] D. C. Brody, Journal of Physics A: Mathematical and Theoretical **47**, 035305 (2013).
 - [116] O. A. Castro-Alvaredo and A. Fring, Journal of Physics A: Mathematical and Theoretical **42**, 465211 (2009).
 - [117] F. Kleefeld, The construction of a general inner product in non-hermitian quantum theory and some explanation for the nonuniqueness of the c operator in pt quantum mechanics (2009), arXiv:0906.1011.
 - [118] F. Bagarello, R. Passante, and C. Trapani, eds., *Non-Hermitian Hamiltonians in Quantum Physics* (Springer International Publishing, 2016).
 - [119] N. Moiseyev, *Non-Hermitian Quantum Mechanics* (Cambridge University Press, 2009).
 - [120] B.-B. Wei and L. Jin, Scientific Reports **7**, 10.1038/s41598-017-07344-z (2017).
 - [121] R. Streubel, P. Fischer, F. Kronast, V. P. Kravchuk, D. D. Sheka, Y. Gaidei, O. G. Schmidt, and D. Makarov, Journal of Physics D: Applied Physics **49**, 363001 (2016).
 - [122] N. Schine, A. Ryou, A. Gromov, A. Sommer, and J. Simon, Nature **534**, 671 (2016).
 - [123] A. J. Kollár, M. Fitzpatrick, and A. A. Houck, Nature **571**, 45 (2019).
 - [124] A. Greenleaf, Y. Kurylev, M. Lassas, and G. Uhlmann, Phys. Rev. Lett. **99**, 183901 (2007).
 - [125] M. P. López-Sancho, F. de Juan, and M. A. H. Vozmediano, Phys. Rev. B **79**, 075413 (2009).